The Journal of Physiological Sciences (2019) 69:661–671
https://doi.org/10.1007/s12576-019-00683-8

ORIGINAL PAPER

# Renal involvement in the pathogenesis of mineral and bone disorder in dystrophin-deficient mdx mouse

Eiji Wada[1,2] · Takayuki Hamano[3] · Isao Matsui[3] · Mizuko Yoshida[2] · Yukiko K. Hayashi[1] · Ryoichi Matsuda[2,4]

Received: 6 March 2019 / Accepted: 30 April 2019 / Published online: 11 May 2019


## Abstract

Duchenne muscular dystrophy is a severe muscular disorder, often complicated with osteoporosis, and impaired renal function has recently been featured. We aimed to clarify the involvement of renal function in the pathogenesis of mineral and bone disorder in mdx mice, a murine model of the disease. We clearly revealed renal dysfunction in adult mdx mice, in which dehydration and hypercalcemia were contributed. We also examined the effects of dietary phosphorus (P) overload on phosphate metabolism. Serum phosphate and parathyroid hormone (PTH) levels were significantly increased in mdx mice by dietary P in a dose-dependent manner; however, bone alkaline phosphatase levels were significantly lower in mdx mice. Additionally, bone mineral density in mdx mice were even worsened by increased dietary P in a dose-dependent manner. These results suggested that the uncoupling of bone formation and resorption was enhanced by skeletal resistance to PTH due to renal failure in mdx mice.

**Keywords** Duchenne muscular dystrophy · Renal dysfunction · Mineral and bone disorder · Osteoporosis · Phosphate overloading

## Introduction

Duchenne muscular dystrophy (DMD) is an X-linked muscular disorder affecting about one in 3500 boys [1]. DMD is caused by deficiency of dystrophin, which is a large 427-kDa protein composed of 3865 amino acid residues that connects the cytoskeleton and basal lamina of skeletal and cardiac muscles [2]. Although there is no effective curable remedy for DMD, patients can live longer with advancements of physical, cardiac, and pulmonary treatments [3, 4]. As a result of increased life expectancy, a variety of dysfunctions of other organs often impair the quality of life of the patients.

Low bone mineral density (BMD) and resultant fracture are major complications in DMD from early stages of the disease [5]. Approximately, one-third of DMD patients suffer from osteoporosis in long bone and/or vertebral bone. They are also at high risk of fractures, which lead to decreased mobility and quality of their life [6]. Multiple factors can lead to low bone mass in DMD, including decreased activity of daily living, low muscle mass, and impaired bone remodeling. As the kidney plays an important role in mineral metabolism, the relationship between renal dysfunction and bone health has been well studied in kidney diseases. Both men and women with chronic kidney disease (CKD) have low BMD, which is a strong risk factor for subsequent fracture [7]. Also, disorders of mineral and bone metabolism are serious complications associated with morbidity and mortality of CKD patients [8]. However, the involvement of renal function in bone health of DMD is not understood.

Renal dysfunction has recently been reported as a frequent complication with the progression of DMD. A Japanese group reveals that 14% of the total death of 286 DMD

**Electronic supplementary material** The online version of this article (https://doi.org/10.1007/s12576-019-00683-8) contains supplementary material, which is available to authorized users.

✉ Eiji Wada
ewada@tokyo-med.ac.jp

1 Department of Pathophysiology, Tokyo Medical University, 6-1-1 Shinjuku, Shinjuku, Tokyo 160-8402, Japan

2 Graduate School of Arts and Sciences, The University of Tokyo, 3-8-1 Komaba, Meguro, Tokyo 153-8902, Japan

3 Department of Comprehensive Kidney Disease Research, Osaka University Graduate of School Medicine, B6-2-2 Yamadaoka, Suita, Osaka 565-0871, Japan

4 Graduate School of Science, Tokyo University of Science, 1-3 Kagurazaka, Shinjuku, Tokyo 162-8601, Japan

patients can be attributed to renal failure, and approximately 30% of patients over the age of 30 have high plasma cystatin C levels, a reliable marker of renal function, which is independent of muscle mass and hydration [9]. It is well known that serum creatinine levels are not reliable for assessing renal function of muscular dystrophies because reduced muscle mass directly affects its levels [10]. Also, mild renal failure is concerned as a treatable complication in DMD since renal function of non-ambulatory DMD patients who have high serum cystatin C levels, improves by correcting dehydration [11]. Another group reports that the incidence of renal stone development in non-ambulatory adult DMD patients (20.7%, six out of 29 subjects) is higher than that of age-matched non-ambulatory control group (1.5%, one out of 68 subjects) [12].

The dystrophin-deficient mdx mouse is an experimental murine model widely used for the study of DMD [13]. Sharing the same genetic mutation in the dystrophin gene, mdx mice exhibit muscle degeneration, but it is compensated by their greater regenerative capacity of muscle fibers than that of human. Muscle degeneration and lower mechanical stress due to muscle weakness play a role in lower bone quality of both DMD patients and mdx mice [14, 15]. However, even young mdx mice (21-day-old) already have low bone mineral content and bone mass before the onset of significant muscle damage in the quadriceps [16]. Therefore, different mechanisms for low bone mass might exist other than muscular dystrophy by the lack of dystrophin.

In this study, we evaluated renal function in mdx mice. Since high phosphate intake is a well-known contributor to the progression of CKD and bone loss, we also clarified the relationship between bone metabolism and renal function of mdx mice fed high-phosphorus (P), normal-P, and low-P diets.

## Materials and methods

### Animal care

Dystrophin-deficient mice (C57BL/10ScSn-mdx: mdx) and wild-type mice (C57BL/10ScSn: B10) were housed in cages with pulp bedding (Palmas-μ; Material Research Center, Tokyo, Japan) in a climate-controlled room with a 12-h light/dark cycle and a temperature of 25 °C. Mice were freely accessed to experimental diet and water. Male mice were used for this experiment, and body weight of both wild-type and mdx mice were measured soon after being sacrificed. Samples from skeletal muscle, kidneys, and the right tibia were collected at the age of 12 weeks. A kidney weight (wet) was measured after blood sample was collected. All experimental procedures were approved by the Experimental Animal Care and Use Committees of Tokyo Medical University and the University of Tokyo.

### Experimental diets

Experimental P diets were used as previously described [17]. Diets containing a P content of either 0.7 g/100 g (low-P diet), 1.0 g/100 g (normal-P diet), or 2.0 g/100 g (high-P diet) were given to wild-type and mdx mice from weaning. Dietary P levels were modulated by adding monopotassium phosphate and monosodium phosphate for the normal-P and high-P diets. The normal-P diet was the same composition as the commercial CE-2 diet (CLEA Japan, Inc., Tokyo, Japan). The lowest concentration of a P diet used in this study contained 0.7 g P in 100 g when all the diet components of the experimental P diets were modified based on the open formula of the National Institute of Health (NIH) diet (NIH-07; NIH, MD, USA) [17]. Other diet components, including Ca (1.2 g/100 g), were present at the same concentration in all diets. Wild-type and mdx mice used in renal function analyses were fed the standard CE-2 diet.

### Voluntary wheel running

To measure voluntary exercise capacity of wild-type and mdx mice, a running wheel was used as previously described [17]. Briefly, the mice fed the standard CE-2 diet were individually housed in free-spinning running wheel cages designed for mice (SN-450; Shinano, Tokyo, Japan) that contained a running wheel. Mice were allowed to acclimate to the running wheel cage for 3 days and then data for daily wheel rotations were collected for the following 7 days. The average number of rotations per day were compared.

### Serum and urinary biochemistry

Blood was collected between 12:00 pm and 4:00 pm since the levels of bone metabolism markers are affected by circadian rhythm and diet. Serum samples were then separated by incubation at room temperature for 2 h, followed by centrifugation at 3500 rpm for 15 min. To separate plasma sample, blood was immediately mixed with 10% total blood volume of 1 mg/ml EDTA/PBS in a 1.5-ml microtube, and centrifuged at 1200 rpm for 30 min. The separated samples were stored at − 80 °C until needed. To collect urine, a mouse was allowed to acclimate to a mouse metabolic cage (SANSYO Co. LTD., Tokyo, Japan) for 2 days, and urine sample was collected for the next 24 h in fasting condition. Urinary samples were centrifuged at 3500 rpm for 10 min before analysis.

Serum inorganic phosphorus (IP), calcium (Ca), total protein (TP), albumin (ALB), creatinine (CRE), uremic acid (UA), and urea nitrogen (UN), and urinary creatinine

(U-CRE) levels were measured using a biochemistry automatic analyzer (model 7180; Hitachi High-Tech, Tokyo, Japan). ELISA kits were used to measure plasma parathyroid hormone (PTH; Mouse PTH 1-84 ELISA kit; Immutopics, CA, USA), serum fibroblast growth factor-23 (FGF-23; FGF-23 ELISA kit; Kainos Laboratories, Tokyo, Japan), serum bone specific alkaline phosphatase (BALP; mouse BALP ELISA kit; Cusabio, Wuhan, China), serum C-terminal collagen crosslinks (CTx; RatLaps EIA, Immunodiagnostic Systems, Boldon, United Kingdom), and serum cystatin C (mouse/rat cystatin C quantitative ELISA kit; R&D Systems, MN, USA). The ELISA tests were used in accordance with the manufacturer's instructions. Serum cystatin C levels were measured using samples from wild-type and mdx mice fed the CE-2 diet at 3, 6, 9, 12, and 30 weeks of age.

## Hematocrit

Blood samples were obtained from wild-type and mdx mice fed the CE-2 diet using a retro-orbital bleeding technique described previously [18]. Mice were anesthetized by constant exposure to 1.5–2.0% isoflurane gas. Blood was collected from the right retro-orbital venous plexus using a heparin-coated micro-capillary tube (Drummond Scientific Company, PA, USA), and hematocrit was measured from the percentage of red blood cells in the total blood samples after centrifugation at 11,000 rpm for 5 min.

## Histologic analyses

Kidneys from wild-type and mdx mice of the different P diet groups were dissected, embedded in OCT compound, and frozen in liquid nitrogen. Transverse serial sections were collected at 8-μm thickness. Sections were stained with hematoxylin and eosin (H&E) to detect renal abnormalities and ectopic calcification. For immunohistochemistry, sections of frozen kidneys were fixed with 10% formalin/PBS or cold acetone. After blocking, sections were incubated with primary antibodies diluted with 0.5% BSA/PBS for 1 h at 37 °C. Primary antibodies used in this experiment were klotho (KM2076, 1:250; TransGenic Inc., Kumamoto, Japan), NaPi 2a (1:1000), NaPi 2c (1:1000), dystrophin (1:500; Abcam, Cambridge, United Kingdom), utrophin (1:1000), β-dystroglycan (1:1000), and α-sarcoglycan (1:1000). Alexa Fluor 488 secondary antibody (1:1000; Invitrogen, CA, USA) was used for detection. Images were acquired using an epifluorescence microscope (model Axiophot; Carl Zeiss MicroImaging, Inc., Jena, Germany). The NaPi 2a and NaPi 2c antibodies were kindly gifted from Dr. H. Segawa (University of Tokushima, Tokushima, Japan). The utrophin [19], β-dystroglycan and α-sarcoglycan antibodies were generous gifts from Dr. H. Imamura (National Institute of Neuroscience, National Center of Neurology and Psychiatry, Tokyo, Japan).

## Preparation of brush border membrane vesicles (BBMV) of kidneys

Isolation of BBMV was performed using $Mg^{2+}$ precipitation technique described previously [20, 21]. Briefly, freshly dissected kidney was minced and collected in a 2.0-ml microtube. 0.8 ml of BBMV isolation buffer (300 mM D-mannitol, 5 mM EDTA, 15 mM Tris–HCl; pH 7.4, complete mini protease inhibitor cocktail; Roche Diagnosis, Basel, Switzerland) was added, and samples were homogenized using a 25-gauge needle with a syringe following with homogenization by a sonicator. Then, 1.12 ml of 12 mM $MgCl_2$ in milliQ water was added and settled on ice for 15 min. After centrifugation at 15,000 rpm for 30 min, supernatant was removed, and pellet was mixed with a sample buffer containing 300 mM D-mannitol, 16 mM HEPES, 10 mM Tris–HCl; pH 7.5, and complete mini protease inhibitor cocktail.

## Western blotting

Kidney was dissected and smashed after it was frozen in liquid nitrogen. Smashed samples were lysed in sodium dodecyl sulfate (SDS)-sample buffer (50 mM Tris–HCl, 2% SDS, 10% glycerol, 50 mM dithiothreitol, 0.0025% bromophenol blue). Total kidney protein samples and BBMV samples were separated by either 5% or 5–20% gradient SDS-PAGE gels and transferred to polyvinylidene fluoride (PVDF; Millipore, MA, USA) membrane by semi-dry Trans-blot turbo transfer system (Bio-Rad, Hercules, CA, USA). PVDF membranes were blocked with Odyssey blocking solution (LI-COR, NE, USA) for 3 h at room temperature before primary antibodies were applied overnight at 4 °C. After washing with tris-buffered saline with 0.1% Tween 20 (TBST), membranes were incubated with Alexa Fluor 680 secondary antibody (1:2000; Invitrogen, CA, USA) and analyzed by the Odyssey Infrared Imaging System (LI-COR, NE, USA).

The primary antibodies used were as follows: dystrophin, utrophin, β-dystroglycan, GAPDH (Abcam), klotho, NaPi 2a, NaPi 2c, and β-actin (GeneTex, CA, USA), diluted with Odyssey blocking solution.

## X-ray micro-computed tomography observation

Tibia from wild-type and mdx mice fed the three P diets were fixed in 10% formalin/PBS and scanned using a non-invasive animal computed tomography (CT) system (SkyScan-1074; Bruker, Kontich, Belgium). X-ray photographs were reconstructed by NRecon Reconstruction system (Bruker), and bone mineral density (BMD) and bone morphometries were

analyzed using CTAn (v.1.16) and CTVol (v.2.3) software (Bruker).

For measuring renal function, renal excretion of an angiographic agent (Iopamiron 300; Bayer, Leverkusen, Germany) was determined by dynamic CT scanning using Latheta LCT-200 X-ray micro CT scanner (Hitachi Ltd., Tokyo, Japan). Dynamic scan is a method that repeatedly scans the same position of a specimen. Briefly, wild-type and mdx mice were embedded in a 48-mm-diameter holder while under anesthesia induced by constant exposure to 1.5–2.0% isoflurane gas; 100 µl of Iopamiron 300 was injected intravenously outside of the scanner, and a mouse was set in immediately after the injection (it took 90 s before scanning started). CT images were captured at a position between lumber 2 and lumber 3. Repeated CT scanning was performed in three slices for 90 times at 15-s intervals. CT levels of an average of three slices of kidneys were calculated using standard analysis software (v. 3.00).

### Statistical analysis

Results were expressed as means ± SD or the median and range. In cases where the means of wild-type and mdx mice fed the CE-2 diet were compared, differences were determined by the Welch's *t* test. For comparing differences in wild-type and mdx mice either fed CE-2 diet (age-dependent) or each P diet, a two-way factorial ANOVA taking interaction of the two factors (genotype × age or genotype × P diets) into consideration was performed with SPSS Statistics ver. 22 (SPSS, Chicago, IL, USA). Values of cystatin C, intact PTH, FGF23, BALP, and CTx were log transformed before being analyzed for their skewed distributions. Statistical tests were two-sided, and $P$ values ≤ 0.05 were considered statistically significant. (*) represents $P < 0.05$, (**) represents $P < 0.01$, and (***) represents $P < 0.001$.

## Results

### Reduced renal function in adult mdx mice

We examined morphological differences in kidneys of wild-type and mdx mice at the age of 12 weeks. Body weight, wet weight of kidney, and relative kidney volume were similar in the genotypes fed the CE-2 diet (Table 1). Full length of dystrophin (427 kDa) was not detected in kidneys, and the autosomal homologue of dystrophin, utrophin, was detected both in wild-type and mdx mice (Fig. 1a, b). β-Dystroglycan was similarly expressed and α-sarcoglycan was not detected in kidneys of the two genotypes (Fig. 1a, b). In addition, we determined the expression of phosphate regulators in kidneys, and found that there were no differences in klotho, NaPi 2a, and NaPi 2c levels in wild-type and mdx mice (Fig. 1c, Supplemental Figure 1).

**Table 1** Characteristic differences in wild-type and mdx mice

| | Wild-type | mdx | *P* value |
|---|---|---|---|
| Body weight (g) | 29.16 ± 1.39 | 29.30 ± 1.97 | 0.86 |
| Kidney weight (mg) | 190 ± 20 | 210 ± 30 | 0.19 |
| Relative kidney volume (%) | 0.67 ± 0.03 | 0.71 ± 0.07 | 0.09 |
| Ca (mg/dl) | 10.82 ± 0.49 | 12.23 ± 0.33 | 0.0001 |
| IP (mg/dl) | 12.11 ± 0.66 | 12.68 ± 0.87 | 0.12 |
| TP (mg/dl) | 4.98 ± 0.20 | 5.51 ± 0.22 | 0.0001 |
| ALB (mg/dl) | 3.10 ± 0.08 | 3.41 ± 0.17 | 0.0001 |
| BUN (mg/dl) | 26.83 ± 3.01 | 30.10 ± 3.29 | 0.03 |
| UA (mg/dl) | 4.94 ± 0.63 | 5.39 ± 0.53 | 0.12 |
| CRE (mg/dl) | 0.126 ± 0.020 | 0.132 ± 0.020 | 0.51 |
| U-CRE (mg/dl) | 14.04 ± 5.83 | 14.64 ± 2.88 | 0.78 |
| Ccr | 113.28 ± 49.27 | 112.79 ± 25.03 | 0.98 |
| Urine volume (ml/day) | 1.2 ± 0.8 | 2.3 ± 0.3 | 0.04 |
| Hematocrit (%) | 45.2 ± 2.1 | 48.9 ± 1.1 | 0.01 |
| Activity levels (times/day) | 10357.9 ± 1051.2 | 8657.4 ± 2093.7 | 0.03 |

Values are the mean ± SD ($n = 10$, each group except urinary volume: $n = 4$–5, hematocrit: $n = 5$, and activity levels: $n = 8$–12, each group)

*Ca* calcium, *IP* inorganic phosphate, *TP* total protein, *ALB* albumin, *BUN* blood urea nitrogen, *UA* uremic acid, *CRE* creatinine, *U-CRE* urine creatinine, *Ccr* creatinine clearance

To determine the renal function, we compared serum levels of cystatin C in the age of 3, 6, 9, 12, and 30 weeks of wild-type and mdx mice ($n = 3$–5) fed a standard CE-2 diet (Fig. 1d). In wild-type mice, serum cystatin C levels were decreased in an age-dependent manner; however, mdx mice slightly increased the levels at 9 weeks of age and had significantly higher levels at 12 and 30 weeks of age ($P < 0.001$). There was no relation between serum creatine kinase levels and cystatin C levels in mdx mice (data not shown). We also measured serum levels of TP, ALB, BUN, and UA to ascertain reduced renal function in mdx mice at 12 weeks of age. Serum TP, ALB, and BUN were significantly higher in mdx mice than wild-type mice (Table 1). Serum and urinary creatinine levels were not different in wild-type and mdx mice that results in similar creatinine clearance rate (Table 1). We measured renal function of wild-type and mdx mice at 12 weeks of age by a novel method using a dynamic scan by Latheta LCT-200. After about 700 s from when a trial started, micro CT levels at slices of a kidney were gradually decreased, and all of the wild-type mice ($n = 4$) excreted the angiographic agent to the same levels (Fig. 1e). On the other hand, the angiographic agent was remained in kidney of most of mdx mice (3 in 4 mice) at the time point, which represented reduced renal excretion rate in mdx mice. These

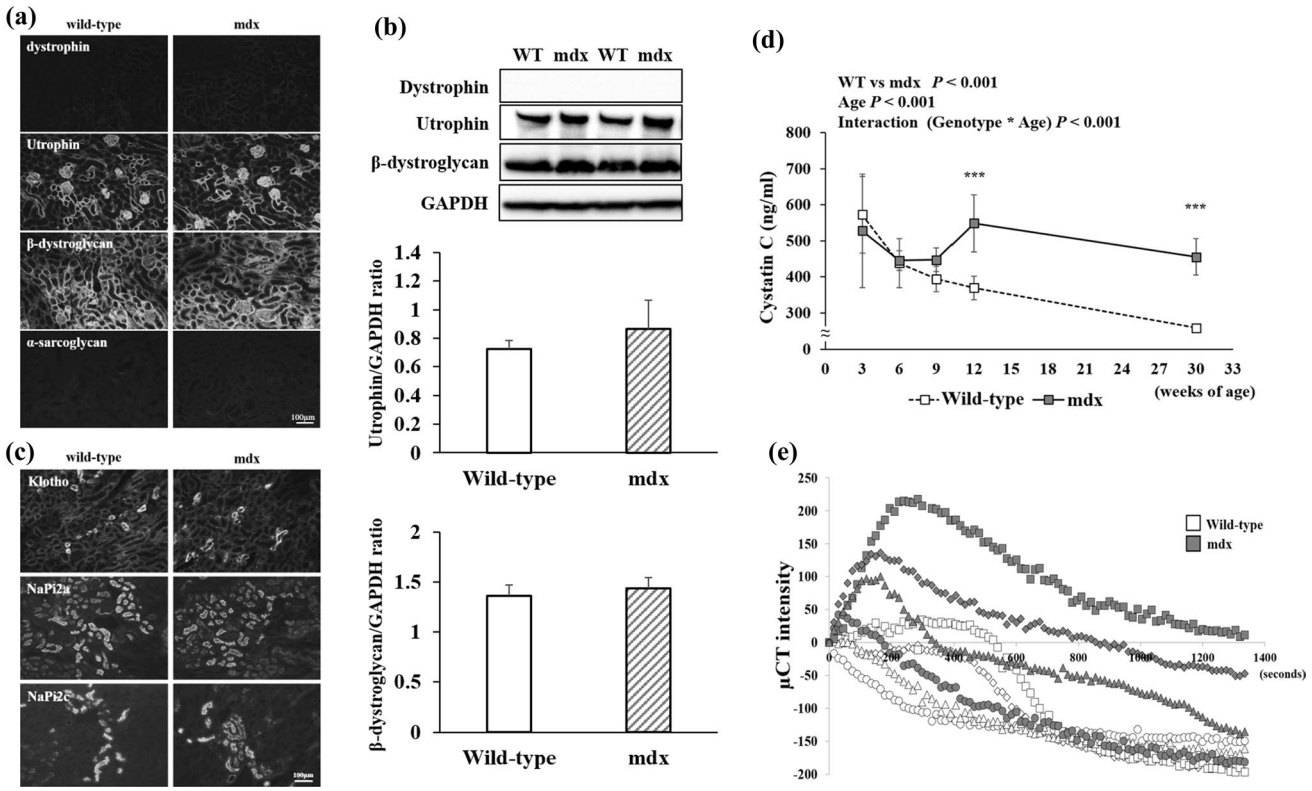


**Fig. 1** Renal function of wild-type and mdx mice. **a** Expressions of dystrophin, utrophin, and dystrophin-related proteins in kidney of wild-type and mdx mice. **b** Western-blot analyses of utrophin and β-dystroglycan. The graph shows quantification of utrophin and β-dystroglycan levels normalized to GAPDH ($n=4$, each group). **c** Expression of klotho, NaPi 2a, and NaPi 2c in the kidney. **d** Detection of cystatin C in serum of wild-type and mdx mice at age 3, 6, 9, 12, and 30 weeks by ELISA ($n=3$-5, each group). Cystatin C levels were significantly increased in mdx mice at 12 and 30 weeks of age. Values of cystatin C are log transformed before analyzed for their skewed distributions; however, the graph and difference are shown in ng/ml. **e** Measurements of renal function using dynamic CT scanning. Renal excretion rate of an angiographic agent was determined by dynamic CT scanning using a micro CT scanner. The results of wild-type mice are plotted in *gray*, and those of mdx mice are plotted in *black* ($n=4$, each group). Renal excretion was delayed in most of mdx mice (three in four mice) after 700 s from a trial started. ***$P<0.001$

results suggested that adult mdx mice have lower renal function than wild-type mice.

## Hypercalcemia and dehydration in mdx mice

Serum Ca levels were significantly increased in mdx mice fed a standard CE-2 diet ($P=0.0001$), and serum IP levels were relatively high in mdx mice (Table 1). The daily urinary volume was significantly increased in mdx mice ($P<0.04$, Table 1), even though daily water consumption was about 7.5 ml in both of the genotypes (data not shown). We also measured the percentage of the volume of red blood cells in whole blood to calculate hematocrit. Wild-type mice had average $45.2\pm2.1\%$ of hematocrit levels and mdx mice had significantly higher levels ($48.9\pm1.1\%$, $P=0.01$, Table 1). These results support that hypercalcemia and dehydration partly contribute to reduced renal function in mdx mice.

## Mineral and bone disorder in mdx mice

To examine phosphate metabolism of wild-type and mdx mice, we used experimental P diets. Serum Ca levels of mdx mice fed the normal-P and high-P diets were significantly higher than those of the diet-matched wild-type mice at age of 90 days ($P<0.01$, Fig. 2a). Dietary P overload significantly reduced serum Ca levels of wild-type mice ($P<0.001$) but the levels of mdx mice remained unchanged by amount of P contents in the diets. Serum levels of IP of wild-type and mdx mice fed either low-P or normal-P diet were not different, but were dramatically increased only in high-P fed mdx mice compared with the diet-matched wild-type mice ($P<0.001$) and mdx mice fed low-P or normal-P diet ($P<0.001$, Fig. 2b). No significant interaction was detected but the difference in the average of serum IP levels in wild-type and mdx mice was increased by dietary P intake in a dose-dependent manner.

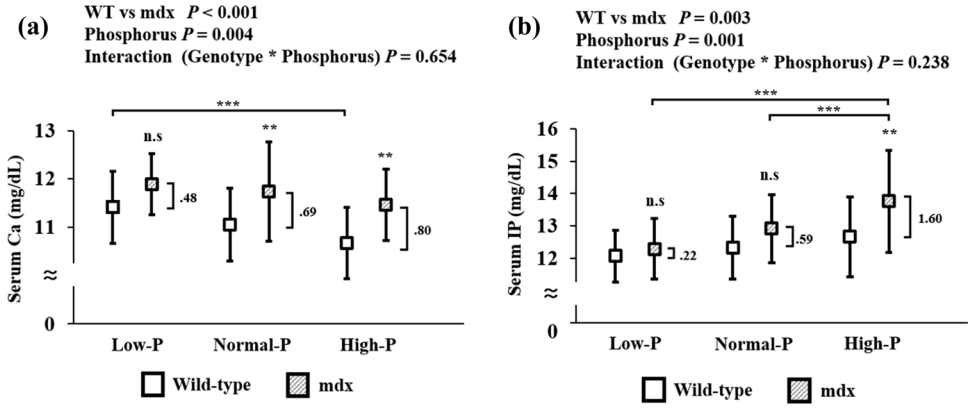


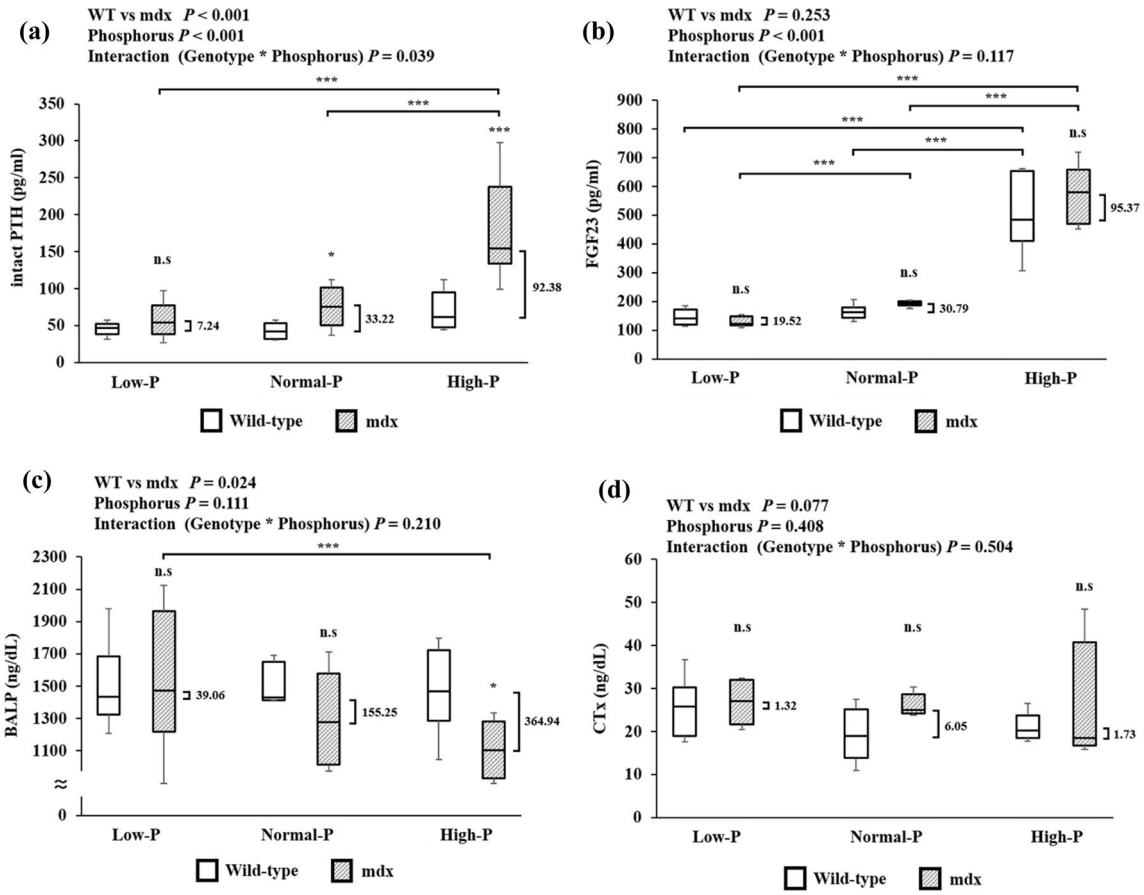


**Fig. 2** Serum levels of calcium and phosphate in mice fed the experimental diets. **a** Serum calcium (Ca) and **b** phosphate (IP) levels are shown as the mean (±SD). Difference in the average of wild-type and mdx mice fed the same diet group is shown in number ($n=18$–21, each group). $^{**}P<0.01$, $^{***}P<0.001$

**Fig. 3** Bone turnover parameters of mice fed the experimental diets. **a** Plasma levels of intact parathyroid hormone (PTH) ($n=5$–6, each group), **b** serum levels of fibroblast growth factor (FGF) 23 ($n=6$–8, each group), **c** bone-specific alkaline phosphatase (BALP) ($n=6$–7, each group) and **d** C-terminal collagen crosslinks (CTx) ($n=5$–6, each group). The data are shown as the interquartile range, with the 75th and 25th percentiles. Difference in the average of wild-type and mdx mice fed the same diet group is shown in numbers. The values are log transformed before being analyzed for their skewed distributions. $^{*}P<0.05$, $^{**}P<0.01$, $^{***}P<0.001$

Intact PTH levels of normal-P fed mdx mice were significantly higher than those of diet-matched wild-type mice and were dramatically increased by dietary P overloading (Fig. 3a). Only in mdx mice did the levels of intact PTH increase as dietary P intake increased, while it remained constant in wild-type mice (interaction $P=0.039$). No significant differences in serum FGF23 levels were observed in wild-type and mdx mice fed the corresponding P diet. Feeding a high-P diet resulted in increases in serum FGF23 levels both in wild-type and mdx mice that were not

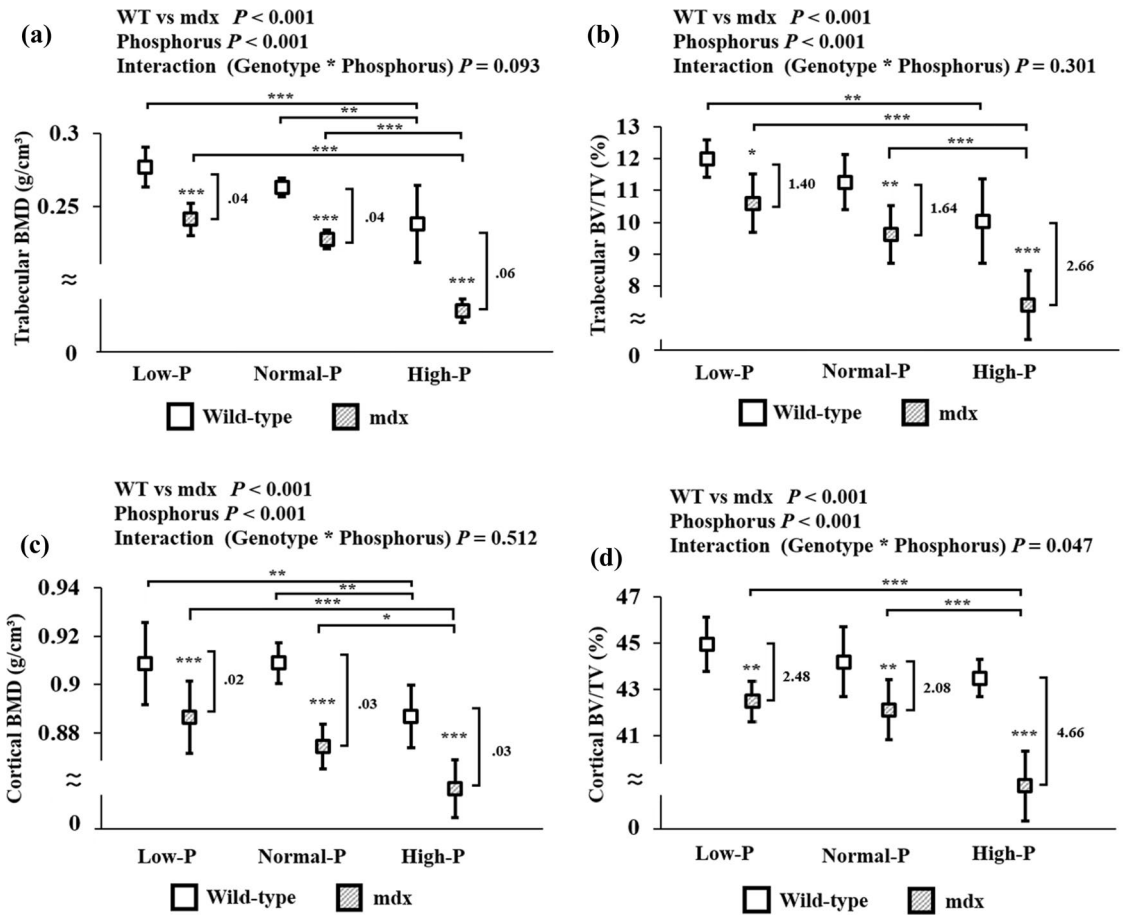


**Fig. 4** Bone phenotype and morphometric parameters of mice fed the experimental diets. **a** Trabecular bone mineral density (BMD), **b** trabecular bone volume (BV)/tissue volume (TV), **c** cortical BMD, and **d** cortical BV/TV. The results are shown as the mean (±SD). Difference in the average of wild-type and mdx mice fed the same diet group is shown in number ($n=4$, each group). $^{*}P<0.05$, $^{**}P<0.01$, $^{***}P<0.001$

significant with no interaction observed between the genotypes (Fig. 3b). In addition, there was no significant difference in levels of klotho, NaPi2a, and NaPi2c expressions in kidney of wild-type and mdx mice fed the same P diet, and those levels were decreased by dietary P overloading (supplemental Figure 1). Dietary P overloading significantly reduced serum BALP levels of mdx mice compared with diet-matched wild-type mice, while no statistically significant differences were found between the genotypes fed either low-P or normal-P diet (Fig. 3c). Serum CTx levels were not different among wild-type and mdx fed the same P diets with no interaction observed (Fig. 3d).

## Dramatic bone mass loss in mdx mice fed high-P diet

The right tibia of wild-type and mdx mice fed the experimental P diet was scanned using an X-ray micro CT scanner, and quantitative morphological parameters for trabecular and cortical bones were evaluated by CTAn and CTVol software. Trabecular BMD was significantly decreased in mdx mice compared with those of wild-type mice, which is independent of the experimental diets; however, high-P diet dramatically worse BMD of mdx mice (interaction $P=0.093$) (Fig. 4a). Trabecular bone volume to tissue volume (BV/TV) ratio was also significantly decreased in mdx mice and was dramatically worsened by a high-P diet (Fig. 4b). Other morphological parameters, such as trabecular bone surface-to-volume ratio (BS/VR) and trabecular number were also significantly affected in mdx mice fed a high-P diet (Supplemental Figure 2). Trabecular number, BMD, and BV/TV abnormalities were also found in wild-type mice by prolong dietary P overloading from weaning to adult. Similar to trabecular bone, cortical bone abnormalities were more prominent in mdx mice compared with wild-type mice, which is independent of the experimental diets. Cortical BMD and BV/TV ratios were also significantly reduced in mdx mice, and dietary P overloading enhanced BMD

abnormality both in wild-type and mdx mice (Fig. 4c). Cortical BV/TV ratio was dramatically reduced in high-P-fed mdx mice compared with diet-matched wild-type mice and mdx mice fed the other P diets with significant interaction observed ($P=0.047$) (Fig. 4d). Cortical mean total cross-sectional area (CSA) was significantly reduced in mdx mice compared with wild-type mice and was only altered in mdx mice by dietary P overloading (Supplemental Figure 2). Another criterion, cortical cross-sectional thickness (CST), was also significantly changed both in wild-type and mdx mice by high-P intake (Supplemental Figure 2). In all bone criteria except cortical BMD, the difference between average of wild-type and mdx mice, as shown on the right side of the boxes in each P diet, was gradually increased with increasing dietary P intake.

## Discussion

In addition to osteoporosis and fracture as major complications in patients with DMD [22, 23], recent studies demonstrate that DMD patients are at a risk of reduced renal function, which is frequent, especially in patients with an advanced stage of the disease [9, 11, 24]. The murine model of DMD, mdx mice have been studied for decades; however, kidney function was not fully determined previously. Our results suggest that mdx mice have reduced renal function, as shown in significantly higher serum cystatin C levels and other serum renal parameters. The renal function test showed reduction of renal excretion rate in mdx mice. Since serum creatinine levels are not reliable for assessing renal function of muscular dystrophies, serum cystatin C levels are now considered as a suitable measurement [10] both in DMD patients and mdx mice. We detected relatively high serum IP levels in mdx mice ($P=0.12$) in this study, and several studies also mention higher serum IP levels in young mdx mice compared with wild-type mice [25, 26]. This will be the first report to evaluate renal function of a murine model of muscular dystrophies using a dynamic scan by a whole-body X-ray micro CT scanner. All of the wild-type mice ($n=4$) excreted the angiographic agent; however, the agent remained in the kidneys of most of the mdx mice ($n=3$ out of 4) after 700 s from when a scan was started. Delayed approach to the peak of micro CT intensity at the given time in kidney of mdx mice indicated a possible interruption in blood circulation in mdx mice.

Dystrophin is expressed in healthy vascular smooth muscles, and lack of the cytoskeletal protein in vessels leads to abnormal vascular functions and reduced angiogenesis in mdx mice [27]. Moreover, the decreased intestinal transit and the fecal output were reported in mdx mice [28]. In our results, histological abnormality was not observed in kidney by H&E staining and immunohistochemistry, and the wet weight of kidney was not different in wild-type and mdx mice. Kidney expresses dystrophin-glycoprotein complex (DGC) such as isoforms of dystrophin, utrophin, dystroglycan, syntrophin, and dystrobrevin [29], which are similarly expressed in wild-type and mdx mice. No obvious histological abnormalities appearing even in dystrophin and utrophin double knock out mouse [30] suggesting that reduced renal function in mdx mice is not directly caused by lack of dystrophin. Recently, renal function of other muscular dystrophies has been examined that renal dysfunction is rare in patients with Fukuyama congenital muscular dystrophy [31] but is a common complication in myotonic dystrophy 1 [32, 33]. Further studies are needed to compare and to elucidate common causal factors of renal dysfunction in muscular dystrophies.

Hypercalcemia and dehydration are related to reduced renal function [34, 35]. We thought to determine how hypercalcemia and dehydration occur in mdx mice and the relationship between those symptoms and renal function. In this study, serum Ca levels were shown to significantly elevate in mdx mice ($P<0.0001$). This result is in agreement with a previous report [36]. Young DMD patients without steroid treatment also have relatively high serum Ca and IP levels (upper limit of normal range) [22] so that higher serum Ca levels seem to be a common symptom related to DMD. Decreased voluntary activity levels in mdx mice ($P=0.03$) suggests that reduced activity due to prolonged muscle degeneration plays a role in pathogenesis of hypercalcemia. Hypercalcemia leads to a significant increase in the volume of urinary excretion in mdx mice while daily water consumption was similar to that of wild-type mice. As predicted, we observed significantly elevated hematocrit values in mdx mice due to dehydration. The other study also reports the increase in hematocrit levels in mdx mice in which the relative values of wild-type and mdx mice are similar to our results [37]. Therefore, our study suggests that potential causal factors of renal dysfunction in mdx mice are hypercalcemia and dehydration.

Dietary P overloading has been reported to increase the risk of vascular calcification and to decrease bone quality of CKD model animals [38–40]. In this study, the effects of dietary P intake on bone and mineral metabolisms in mdx mice were determined. In wild-type mice, levels of serum Ca were significantly decreased while serum IP levels were unaffected by increasing dietary P intake; however, serum Ca levels remained high and serum IP levels were dramatically increased in mdx mice by dietary P in a dose-dependent manner. This result indicates that mdx mice are susceptible to prolonged P overload due to reduced renal function.

Physiologic phosphate homeostasis is controlled by a feedback system of multiple organs. The main regulators of serum IP are bone-derived FGF-23, PTH secreted from parathyroid gland, and renal phosphate transporters (klotho,

NaPi 2a, and NaPi 2c) [41, 42]. FGF-23 reduces serum IP levels by suppressing re-absorption of phosphate in the renal tubules, and PTH also works to reduce re-absorption of phosphate in the kidney. Klotho is first reported as an aging-suppressor gene and is secreted principally in distal tubules to participate in phosphate metabolism [43]. FGF-23 knockout (KO) and klotho KO mice are reported to exhibit similar pathologic phenotypes such as premature aging, osteoporosis, hyperphosphatemia, and vascular calcification [43, 44]. NaPi 2a and NaPi 2c are two important phosphate co-transporters in proximal tubules of the kidney. It has been clarified that PTH, FGF-23, and klotho directly suppress NaPi 2a and NaPi 2c-dependent phosphate uptake in proximal tubules [45].

Our data demonstrate that mdx mice have abnormal bone and mineral metabolisms and are highly susceptible to dietary P overloading due to reduced renal function. In a normal-P diet, mdx mice have significantly high PTH levels and relatively high serum FGF-23 levels. Secretion of PTH increases in response to low serum Ca levels, and its production stimulates to release Ca from bone (resorption). On the other hand, previous studies clearly demonstrate that in addition to the catabolic role of PTH in bone metabolism, PTH has an anabolic effect on bone [46, 47]. Also, high phosphate concentration directly stimulates secretion of PTH [48]. In a normal-P diet, both serum levels of BALP and CTx of mdx mice were similar to those of wild-type mice. In mdx mice, serum PTH and FGF-23 levels were significantly increased, and serum BALP were significantly decreased by dietary P in a dose-dependent manner. Serum PTH and BALP levels of high-P-fed mdx mice were significantly different compared to those of diet-matched wild-type mice even though serum Ca levels were significantly high. There was no significant difference in levels of klotho, NaPi2a, and NaPi2c expression in kidney of wild-type and mdx mice fed the same P diet, and those levels were decreased by dietary P overloading. Therefore, renal-PTH resistance in mdx mice induced bone uncoupling, which was enhanced by dietary P overloading.

In adult mdx mice, low BMD and impaired bone remodeling are reported in several studies. Compared with wild-type mice, mdx mice have significantly reduced BMD in both trabecular and cortical bones, and serum CTx is elevated [14]. The other study shows that chronic inflammation related to muscle necrosis deteriorates bone loss and delayed bone regeneration in adult mdx mice [15]. However, young mdx mice (21-day-old) already have lowered mineral content and reduced bone morphometric parameters in femur before onset of muscle degeneration in quadriceps muscle [16]. These studies indicate that primary and/or secondary effect(s) of dystrophin deficiency is (are) related to bone loss in mdx mice. In addition, excessive dietary phosphorus/phosphate intake is a risk of impaired bone health in experimental animals and general population [40, 49–51]. For instance, a dramatic reduction in BMD and abnormal bone morphometric parameters are seen in mice with CKD fed a high-phosphate diet [39]. Wild-type mice fed a high-P diet also reduced trabecular and cortical BMD, and we predicted that prolonged dietary P overload from weaning affects to bone health even in wild-type mice especially during a growth period. In mdx mice, dramatic muscle degeneration and immobilization play a role in hypercalcemia, and renal dysfunction is partly triggered by the two causal factors. We revealed that renal-PTH resistance is present in mdx mice, which induces uncoupling of bone formation. Moreover, dietary P overload exacerbated bone quality of mdx mice in which renal-PTH-induced bone uncoupling plays a role in accelerating osteoporosis in the DMD model (Fig. 5).

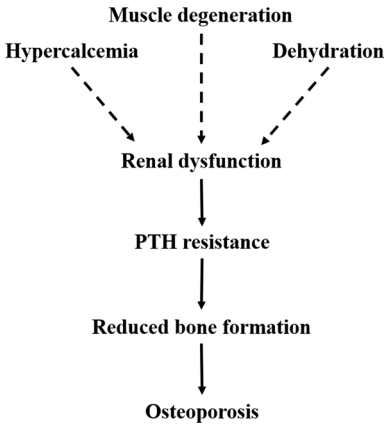


**Fig. 5** Schematic model indicating the mineral and bone disorder in mdx mice. Dramatic muscle degeneration and immobilization play a role in hypercalcemia, and renal dysfunction is partly triggered by hypercalcemia and dehydration. Renal dysfunction and increased PTH levels contribute to lower bone density in adult mdx mice

## Conclusions

Our study clearly demonstrated that dietary P overload exacerbates musculoskeletal health in mdx mice, and renal dysfunction as a new complication, is partly occurred by hypercalcemia and related to muscular dystrophy. Reduced renal function might be a non-specific complication by the lack of dystrophin gene. The uncoupling of bone formation and resorption was enhanced by skeletal resistance to PTH due to renal failure in mdx mice. Taken together, renal dysfunction contributes to mineral and bone disorder in muscular dystrophy, which is susceptible to dietary P overload. This study gives new insight into the relationship between renal function and musculoskeletal health in DMD.

**Acknowledgements** We thank Dr. Michihiro Imamura at National Institute of Neuroscience, National Center of Neurology and Psychiatry and Dr. Hiroko Segawa at University of Tokushima for providing the antibodies. We also thank Mr. Shinsuke Kimura at Hitachi Ltd. for his technical support.

**Author contributions** EW designed the study, performed experiments, analyzed the data, and drafted the manuscript. TH designed the study, especially in statistical analysis. IM and MY analyzed the data, and YH and RM designed and supervised the study and helped to draft the manuscript. All authors read and approved the final manuscript.

**Funding** Funding was provided by Health and Labour Sciences Research Grant for Comprehensive Research on Disability Health and Welfare (H22-016), Intramural Research Grant (29-4) for Neurological and Psychiatric Disorders of NCNP, Grant-in aid from the Ministry of Education, Culture, Sports, Science and Technology of Japan (25650106), Research Grant from Tokyo Medical University (H30). MEXT-Supported Program for the Strategic Research Foundation at Private Universities.

## Compliance with ethical standards

**Conflict of interest** All authors declare that they have no conflicts of interest.

## References

1. Moser H (1984) Duchenne muscular dystrophy: pathogenetic aspects and genetic prevention. Hum Genet 66(1):17–40
2. Hoffman EP, Brown RH, Kunkel LM (1987) Dystrophin: the protein product of the Duchenne muscular dystrophy locus. Cell 51(6):919–928
3. Villanova M, Brancalion B, Mehta AD (2014) Duchenne muscular dystrophy: life prolongation by noninvasive ventilatory support. Am J Phys Med Rehabil 93(7):595–599
4. Liew WK, Kang PB (2013) Recent developments in the treatment of Duchenne muscular dystrophy and spinal muscular atrophy. Ther Adv Neurol Disord 6(3):147–160
5. Pouwels S, de Boer A, Leufkens HG, Weber WE, Cooper C, van Onzenoort HA et al (2014) Risk of fracture in patients with muscular dystrophies. Osteoporos Int 25(2):509–518
6. James KA, Cunniff C, Apkon SD, Mathews K, Lu Z, Holtzer C et al (2015) Risk factors for first fractures among males with Duchenne or Becker muscular dystrophy. J Pediatr Orthop 35(6):640–644
7. West SL, Lok CE, Langsetmo L, Cheung AM, Szabo E, Pearce D et al (2015) Bone mineral density predicts fractures in chronic kidney disease. J Bone Miner Res 30(5):913–919
8. Kestenbaum B, Sampson JN, Rudser KD, Patterson DJ, Seliger SL, Young B et al (2005) Serum phosphate levels and mortality risk among people with chronic kidney disease. J Am Soc Nephrol 16(2):520–528
9. Matsumura T, Saito T, Fujimura H, Sakoda S (2012) Renal dysfunction is a frequent complication in patients with advanced stage of Duchenne muscular dystrophy. Rinsho Shinkeigaku 52(4):211–217
10. Viollet L, Gailey S, Thornton DJ, Friedman NR, Flanigan KM, Mahan JD et al (2009) Utility of cystatin C to monitor renal function in Duchenne muscular dystrophy. Muscle Nerve 40(3):438–442
11. Motoki T, Shimizu-Motohashi Y, Komaki H, Mori-Yoshimura M, Oya Y, Takeshita E et al (2015) Treatable renal failure found in non-ambulatory Duchenne muscular dystrophy patients. Neuromuscul Disord 25(10):754–757
12. Shumyatcher Y, Shah TA, Noritz GH, Brouhard BH, Spirnak JP, Birnkrant DJ (2008) Symptomatic nephrolithiasis in prolonged survivors of Duchenne muscular dystrophy. Neuromuscul Disord 18(7):561–564
13. Bulfield G, Siller WG, Wight PA, Moore KJ (1984) X chromosome-linked muscular dystrophy (mdx) in the mouse. Proc Natl Acad Sci USA 81(4):1189–1192
14. Rufo A, Del Fattore A, Capulli M, Carvello F, De Pasquale L, Ferrari S et al (2011) Mechanisms inducing low bone density in Duchenne muscular dystrophy in mice and humans. J Bone Miner Res 26(8):1891–1903
15. Abou-Khalil R, Yang F, Mortreux M, Lieu S, Yu YY, Wurmser M et al (2014) Delayed bone regeneration is linked to chronic inflammation in murine muscular dystrophy. J Bone Miner Res 29(2):304–315
16. Nakagaki WR, Bertran CA, Matsumura CY, Santo-Neto H, Camilli JA (2011) Mechanical, biochemical and morphometric alterations in the femur of mdx mice. Bone 48(2):372–379
17. Wada E, Yoshida M, Kojima Y, Nonaka I, Ohashi K, Nagata Y et al (2014) Dietary phosphorus overload aggravates the phenotype of the dystrophin-deficient mdx mouse. Am J Pathol 184(11):3094–3104
18. Sharma A, Fish BL, Moulder JE, Medhora M, Baker JE, Mader M et al (2014) Safety and blood sample volume and quality of a refined retro-orbital bleeding technique in rats using a lateral approach. Lab Anim (NY) 43(2):63–66
19. Imamura M, Ozawa E (1998) Differential expression of dystrophin isoforms and utrophin during dibutyryl-cAMP-induced morphological differentiation of rat brain astrocytes. Proc Natl Acad Sci USA 95(11):6139–6144
20. Biber J, Stieger B, Stange G, Murer H (2007) Isolation of renal proximal tubular brush-border membranes. Nat Protoc 2(6):1356–1359
21. Breusegem SY, Takahashi H, Giral-Arnal H, Wang X, Jiang T, Verlander JW et al (2009) Differential regulation of the renal sodium-phosphate cotransporters NaPi-IIa, NaPi-IIc, and PiT-2 in dietary potassium deficiency. Am J Physiol Renal Physiol 297(2):F350–F361
22. Bianchi ML, Morandi L, Andreucci E, Vai S, Frasunkiewicz J, Cottafava R (2011) Low bone density and bone metabolism alterations in Duchenne muscular dystrophy: response to calcium and vitamin D treatment. Osteoporos Int 22(2):529–539
23. Cohran VC, Griffiths M, Heubi JE (2008) Bone mineral density in children exposed to chronic glucocorticoid therapy. Clin Pediatr (Phila) 47(5):469–475
24. Villa CR, Kaddourah A, Mathew J, Ryan TD, Wong BL, Goldstein SL et al (2016) Identifying evidence of cardio-renal syndrome in patients with Duchenne muscular dystrophy using cystatin C. Neuromuscul Disord. 26(10):637–642
25. Kikkawa N, Ohno T, Nagata Y, Shiozuka M, Kogure T, Matsuda R (2009) Ectopic calcification is caused by elevated levels of serum inorganic phosphate in mdx mice. Cell Struct Funct 34(2):77–88
26. Brazeau GA, Mathew M, Entrikin RK (1992) Serum and organ indices of the mdx dystrophic mouse. Res Commun Chem Pathol Pharmacol 77(2):179–189
27. Ito K, Kimura S, Ozasa S, Matsukura M, Ikezawa M, Yoshioka K et al (2006) Smooth muscle-specific dystrophin expression improves aberrant vasoregulation in mdx mice. Hum Mol Genet 15(14):2266–2275
28. Mulè F, Amato A, Serio R (2010) Gastric emptying, small intestinal transit and fecal output in dystrophic (mdx) mice. J Physiol Sci. 60(1):75–79

29. Loh NY, Newey SE, Davies KE, Blake DJ (2000) Assembly of multiple dystrobrevin-containing complexes in the kidney. J Cell Sci 113(Pt 15):2715–2724
30. Rafael JA, Trickett JI, Potter AC, Davies KE (1999) Dystrophin and utrophin do not play crucial roles in nonmuscle tissues in mice. Muscle Nerve 22(4):517–519
31. Ishigaki K, Kato I, Murakami T, Sato T, Shichiji M, Ishiguro K et al (2019) Renal dysfunction is rare in Fukuyama congenital muscular dystrophy. Brain Dev 41(1):43–49
32. Matsumura T, Saito T, Yonemoto N, Nakamori M, Sugiura T, Nakamori A et al (2016) Renal dysfunction can be a common complication in patients with myotonic dystrophy 1. J Neurol Sci 368:266–271
33. Aldenbratt A, Lindberg C, Svensson MK (2017) Reduced renal function in patients with Myotonic Dystrophy type 1 and the association to CTG expansion and other potential risk factors for chronic kidney disease. Neuromuscul Disord 27(11):1038–1042
34. Komatsu Y, Imai Y, Itoh F, Kojima M, Isaji M, Shibata N (2005) Rat model of the hypercalcaemia induced by parathyroid hormone-related protein: characteristics of three bisphosphonates. Eur J Pharmacol 507(1–3):317–324
35. Daily JW, Zhang T, Wu X, Park S (2019) Chronic water insufficiency induced kidney damage and energy dysregulation despite reduced food intake, which improved gut microbiota in female rats. J Physiol Sci. https://doi.org/10.1007/s12576-019-00668-7
36. Glesby MJ, Rosenmann E, Nylen EG, Wrogemann K (1988) Serum CK, calcium, magnesium, and oxidative phosphorylation in mdx mouse muscular dystrophy. Muscle Nerve 11(8):852–856
37. Mosqueira M, Baby SM, Lahiri S, Khurana TS (2013) Ventilatory chemosensory drive is blunted in the mdx mouse model of Duchenne muscular dystrophy (DMD). PLoS One 8(7):e69567
38. Lau WL, Leaf EM, Hu MC, Takeno MM, Kuro-o M, Moe OW et al (2012) Vitamin D receptor agonists increase klotho and osteopontin while decreasing aortic calcification in mice with chronic kidney disease fed a high phosphate diet. Kidney Int 82(12):1261–1270
39. Lau WL, Linnes M, Chu EY, Foster BL, Bartley BA, Somerman MJ et al (2013) High phosphate feeding promotes mineral and bone abnormalities in mice with chronic kidney disease. Nephrol Dial Transplant 28(1):62–69
40. Huttunen MM, Tillman I, Viljakainen HT, Tuukkanen J, Peng Z, Pekkinen M et al (2007) High dietary phosphate intake reduces bone strength in the growing rat skeleton. J Bone Miner Res 22(1):83–92
41. Kuro-o M (2010) Overview of the FGF23-Klotho axis. Pediatr Nephrol 25(4):583–590
42. Lanske B, Razzaque MS (2014) Molecular interactions of FGF23 and PTH in phosphate regulation. Kidney Int 86(6):1072–1074
43. Kuro-o M, Matsumura Y, Aizawa H, Kawaguchi H, Suga T, Utsugi T et al (1997) Mutation of the mouse klotho gene leads to a syndrome resembling ageing. Nature 390(6655):45–51
44. DeLuca S, Sitara D, Kang K, Marsell R, Jonsson K, Taguchi T et al (2008) Amelioration of the premature ageing-like features of Fgf-23 knockout mice by genetically restoring the systemic actions of FGF-23. J Pathol 216(3):345–355
45. Meir T, Durlacher K, Pan Z, Amir G, Richards WG, Silver J et al (2014) Parathyroid hormone activates the orphan nuclear receptor Nurr1 to induce FGF23 transcription. Kidney Int 86(6):1106–1115
46. Lombardi G, Di Somma C, Rubino M, Faggiano A, Vuolo L, Guerra E et al (2011) The roles of parathyroid hormone in bone remodeling: prospects for novel therapeutics. J Endocrinol Investig 34(7 Suppl):18–22
47. Iida-Klein A, Zhou H, Lu SS, Levine LR, Ducayen-Knowles M, Dempster DW et al (2002) Anabolic action of parathyroid hormone is skeletal site specific at the tissue and cellular levels in mice. J Bone Miner Res 17(5):808–816
48. Almaden Y, Hernandez A, Torregrosa V, Canalejo A, Sabate L, Fernandez Cruz L et al (1998) High phosphate level directly stimulates parathyroid hormone secretion and synthesis by human parathyroid tissue in vitro. J Am Soc Nephrol 9(10):1845–1852
49. Kemi VE, Kärkkäinen MU, Lamberg-Allardt CJ (2006) High phosphorus intakes acutely and negatively affect Ca and bone metabolism in a dose-dependent manner in healthy young females. Br J Nutr 96(3):545–552
50. Kemi VE, Rita HJ, Kärkkäinen MU, Viljakainen HT, Laaksonen MM, Outila TA et al (2009) Habitual high phosphorus intakes and foods with phosphate additives negatively affect serum parathyroid hormone concentration: a cross-sectional study on healthy premenopausal women. Public Health Nutr 12(10):1885–1892
51. Huttunen MM, Pietilä PE, Viljakainen HT, Lamberg-Allardt CJ (2006) Prolonged increase in dietary phosphate intake alters bone mineralization in adult male rats. J Nutr Biochem 17(7):479–484